



# NUMERICAL STUDY ON HEAT TRANSFER CHARACTERISTICS OF CORRUGATED TUBE PHASE CHANGE THERMAL ENERGY STORAGE UNIT

Kun Zhang <sup>a,b,\*</sup>, Zhiyong Li <sup>a,b</sup>, Jia Yao <sup>a,b</sup>

<sup>a</sup> School of Mechanical Engineering, Lanzhou Jiaotong University, Lanzhou, Gansu, 730070, China

<sup>b</sup> Key Laboratory of Railway Vehicle Thermal Engineering of MOE, Lanzhou Jiaotong University, Lanzhou, Gansu, 730070, China

## ABSTRACT

Detailed numerical analysis is presented for heat transfer characteristics of charging or discharging process in phase change thermal energy storage unit with inner corrugated tube. The results indicated that the charging or discharging rate of phase change material (PCM) for the case of inner corrugated tube is obviously higher than that in unit with inner plain tube due to the increasing heat transfer surface. The heat transfer rate increase with the increasing mass flow rate. However, when the mass flow rate of heat transfer fluid (HTF) is greater than 0.0315kg/s, the charge and discharge time can not be obviously shorten by increasing mass flow rate. The heat transfer rate between PCM and HTF increases with the increasing of wave amplitude and the decreasing of wavelength.

**Keywords:** Latent heat storage system, Phase change material, Corrugated tube

## 1. INTRODUCTION

Phase change heat storage technologies have been widely used in building thermal regulation, battery thermal management, cold chain transportation, solar thermal system and other areas (Amirante et al., 2017; Kenisarin et al., 2007; Shukla et al., 2009; El-Shaarawi et al., 2012). There has been a growth of interest in the heat transfer characteristics of shell-and-tube phase change heat storage unit because of its high efficiency and relative small volume. Lacroix (1993) studied a theoretical model to predict the transient behavior of a shell-and-tube storage unit with the PCM on the shell side and assess the effects of various geometric parameters on the heat transfer process. Trp (Trp, 2005; Trp et al., 2006) numerically and experimentally studied phase change in a shell-and-tube latent thermal energy storage system with paraffin as the PCM. The HTF is flowing through the tube and the PCM is filled in the shell side. They obtained the operating conditions and geometry optimization by analyzing the influence of several HTF flow rate, inlet temperature and several geometric parameters on the heat transfer process. Rathod and Banerjee (2014) experimentally studied the effect of fluid inlet temperature and mass flow rate on temperature distribution of PCM for both the melting and solidification processes. Hosseini et al. (2012;2014) numerically and experimentally studied the heat transfer rate and thermal behavior of a shell-and-tube heat transfer storage unit filled with RT50 as PCM during charging process. Gong (1996) and Fang et al. (2006) investigated the effect of different multiphase change materials on the performance of shell-and-tube phase change heat storage unit. They found that there is an optimal ratio among multiple phase change materials to obtain the maximum thermal energy charging rate. Therefore, a lot of studies indicated that there are plenty of influencing factors need to be considered for a shell-and-tube phase change storage unit such as geometric parameters, configuration, the thermodynamic property, initial and boundary conditions (Gang et al., 2020; Liang et al., 2020; Yang et al., 2021).

The main disadvantage of shell-and-tube PCM heat storage unit originates from the low thermal conductivity of PCM, which limits the heat transfer rate during charging or discharging processes (Yang et al., 2019; Tao et al., 2017; Kumar et al., 2020). The extended surfaces techniques are considered efficient and relatively simple for improving the heat transfer rate (Maike et al., 2018; Ruihuan et al., 2020; Qi et al., 2019). Esapour et al. (2016) numerically investigated the effect of number of inner tube on the melting process in multi-tube heat exchanger. The obvious reduction of melting time for the case of double inner tube in comparison with the case of single inner tubes. Agyenim et al. (2009) experimentally compared a shell-and-tube configuration with one heat transfer tube and a unit with multi-tubes. They found that the reduced melt time for the multi-tube unit was due to the increased surface area of the multi-tubes unit compared to that of the single tube unit. Some similar conclusions for phase change heat storage unit with multi-tubes have been obtained by other authors (Seong et al., 2020; Qaiser et al., 2021; Kousha et al., 2019). Khalifa et al., (2001) et al. studied a vertical shell-and-tube phase change heat storage unit with axial fins. The use of axial fins has a faster heat transfer rate and higher heat transfer efficiency than without axial fins. Tao et al. (2012) studied the thermal performance of phase change heat storage devices using inner tapered finned tubes and inner spiral finned tubes, respectively. It indicates that the melting time of the three finned tubes is reduced by about 26.9% and 30.7% when it is compared with the case of plain tube. Hosseini et al (2015). experimentally and numerically studied the effect of longitudinal fins in a double pipe heat exchanger with PCM during charging process. The heat transfer rate can be enhanced by attaching the extra fins. All the above results obviously showed that the extended surface area of heat transfer between the wall and PCM can lead to a less melting time and an increasing heat transfer rate. However, most of these above studies in recent years focused on the applications of fins or multi-tubes for improving the heat transfer rate. In fact, the use of corrugated tube of

\* Corresponding author. Email: zhangkun52015@163.com

heat transfer fluid is also an effective way because that the corrugated surface has the function of expanding the heat transfer surface. The advantage of corrugated tube in heat exchanger without PCM has been proved by many authors (Wang et al., 2016; Li et al., 2017; Ding et al 2022). Zhang et al (2020). studied the flow and heat transfer characteristics of xanthan gum solution in corrugated tube and circular tube. They concluded that the corrugated tube is more applicable in energy saving and heat transfer enhancement. Al-Obaid et al (2019) investigated the flow characteristics and enhanced heat transfer in three-dimensional smooth tubes and corrugated tube. The results show that compared with the smooth tube, the corrugated tube has higher heat transfer enhancement under the conditions of a low mass flow of 0.56 L/min and a corrugated ring diameter of 1 mm. When the corrugated ring diameter is 1 mm, 0.5 mm and 0.375 mm, the heat transfer enhancement is 26.48%, 19.43 and 15.26%, respectively. However, little work has been reported on the shell-and-tube phase change heat storage unit with corrugated tube. Mazhar et al. (2021) studied the charging and discharging of heat exchangers with corrugated structures. The use of corrugated tubes improves the heat transfer coefficient and shortens the charge and discharge process of the heat exchanger. Thermal performance factor for this particular corrugated pipe increases by 3.1 for melting and 2.4 for freezing. Yarmohammadi et al. (2016) investigated the flow and heat transfer characteristics of R404A vapor condensation in a corrugated tube. The test is carried out by controlling the flow rate of the fluid of inside tube and outside tube and the condensation temperature. The results demonstrate that the average heat transfer coefficient obtained from the corrugated tubes is noticeably higher than the average heat transfer coefficient obtained from the smooth tube at the same vapor quality. However, these studies have not studied the effects of different wave amplitudes and wavelengths of the corrugated tube on the heat transfer performance of the phase change heat storage unit in detail.

The objective of this paper is to investigate the thermal behavior and performance of shell-and-tube phase change heat storage unit with inner corrugated tube. The influence of wavelength and wave amplitude on the phase change heat storage unit of corrugated tube will be analyzed. Liquid fraction in PCM and heat flow rate between HTF and PCM with time will be calculated to investigate the effect of geometric parameters on the heat transfer process of shell-and-tube phase change heat storage unit.

## 2. PHYSICAL MODEL AND GOVERNING EQUATIONS

### 2.1 Physical model

A schematic diagram of the physical model under consideration is shown in Fig. 1, which is composed of corrugated tube inside a cylindrical envelope forming a shell-and-tube storage unit. The PCM (n-octadecane) is placed into the shell while the heat transfer fluid flows inside the tubes. The inside tube ( $d_i = 12.7$  mm,  $\delta = 1.55$  mm and  $L = 400$  mm long) is made of copper. Water is considered as the HTF which flows through the inner tube and exchanges heat with phase change material. The application of the corrugated tube in the phase change heat storage unit can be regarded as an axisymmetric simplified to a two-dimensional model. The viscous dissipation in the fluid is negligible compared to the convection in the HTF domain and the outer wall of the tube is assumed to be adiabatic.

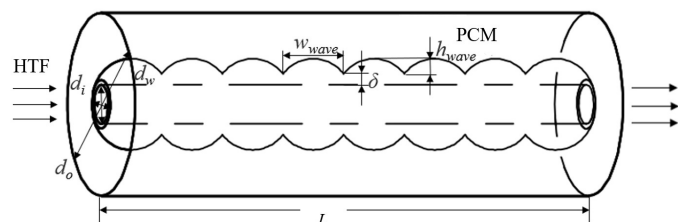


Fig. 1 Schematic diagram of physical model

### 2.2 Governing equations

Numerical method is used to investigate thermal performances of phase change heat transfer. In order to simulate phase change of melting in a shell-and-tube heat storage unit, enthalpy method is used for solving the phase change heat transfer process (Tao et al., 2012; Hosseini et al., 2015). The solid-liquid interface is indicated by a mushy zone which separates the two phase. The energy equation in PCM domain is written as

$$\frac{\partial \rho h}{\partial t} = \nabla \cdot (k \nabla T) - \frac{\partial \rho f H}{\partial t} \quad (1)$$

where  $f$  is the fraction of a cell volume in liquid form,  $H$  is the latent heat and the enthalpy  $h$  is expressed as

$$h = h_{ref} + \int_{T_{ref}}^T c_p dT \quad (2)$$

where  $c_p$  is the specific heat and  $h_{ref}$  is the enthalpy at the reference temperature  $T_{ref}$ . The value of liquid fraction  $\phi$  can be calculated by the following equations:

$$\phi = \begin{cases} 0 & T < T_s \\ \frac{T - T_s}{T_{liq} - T_s} & T_s \leq T \leq T_{liq} \\ 1 & T_{liq} < T \end{cases} \quad (3)$$

The value of liquid fraction  $\phi$  is between 0 and 1. The effect of natural convection is considered by using an effective thermal conductivity in Ref. (Kousha et al., 2019; Ismail et al., 2001). The thermal conductivity of phase change material  $k$  can be expressed as:

$$k = \phi k_e + (1 - \phi) k_p \quad (4)$$

$$k_e / k_{liq} = CRA^n \quad (5)$$

where  $k_e$  is the effective thermal conductivity,  $k_{liq}$  and  $k_s$  represent the thermal conductivity of liquid and solid, respectively. The values of  $C$  and  $n$  in Eq. (5) are 0.099 and 0.24, respectively.

The above equations are solved by a commercial CFD code, ANSYS FLUENT 19.2. The discretization of convection term is with second-order upwind scheme and the SIMPLE scheme is applied for pressure-velocity coupling. The HTF is considered turbulent and incompressible, thus (K- $\epsilon$ ) model is used to solving this flow regime.

The thermo-physical properties of the PCM, inner tube wall and heat transfer fluid are independent of temperature, but the properties of the PCM are different in the liquid and solid phase. The thermal properties of HTF, corrugated tube and PCM are shown in Table 1.

Table 1 Material properties of PCM, HTF and corrugated tube.

	Paraffin C18	Water	Copper
$T_m$ (K)	298.2-300.7	273.15	—
$\rho$ (kg/m <sup>3</sup> )	771	995	8930
$k_{liq}$ (W/(m·K))	0.148	0.62	—
$k_p$ (W/(m·K))	0.358	—	398
$c_p$ J/(kg·K)	2222	—	386
$H$ (J/kg)	243500	—	—
$\mu_{pl}$ (kg/(m·s))	0.003094	0.000769	—
$\beta$ (1/K)	0.0009	—	—

### 3. NUMERICAL METHOD AND ITS VALIDATION

The grid-independence of the numerical results is studied for the charging process with mass flow rate of HTF  $q_m = 0.0315$  kg/s, initial temperature  $T_0 = 282.7$  K, inlet temperature  $T_{in} = 310.7$  K and material properties shown in Table 1. The wave length and amplitude of corrugated tube are  $h_{wave} = 16$ mm and  $w_{wave} = 1$ mm, respectively. The time step is varied from 1 s to 0.02 s, and the value of 0.05 s is chosen based on precision and computational time. When the time step is equal to 0.1, the five grid sizes in Table 2 are used to complete the grid-independence study. It is noted that the total numbers of grid points for the five meshes size are  $32 \times 700$ ,  $45 \times 1000$ ,  $57 \times 1300$ ,  $100 \times 1800$  and  $130 \times 2700$ , respectively. Numerical results indicated that the relative error of liquid fraction corresponding to a grid number of  $100 \times 1800$  and  $130 \times 2700$  is less than 1%;  $100 \times 1800$  grid points are adequate to yield accurate results. In order to get high resolution, the grid lines are more closely packed nearby the inner tube wall. Fig. 2 shows the grid system in the middle of the total computational domain.

**Table 2** Liquid fractions at  $\tau = 5$  min for different grid numbers

Grid	$32 \times 700$	$45 \times 1000$	$57 \times 1300$	$100 \times 1800$	$130 \times 2700$
Liquid fraction	0.520	0.468	0.636	0.578	0.575

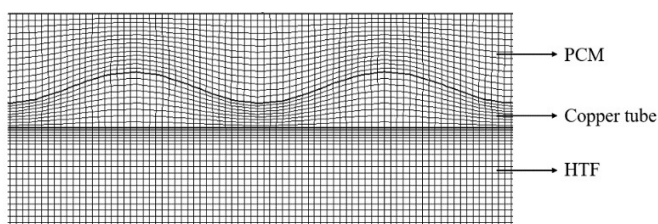


**Fig. 2** Sample of grid system in the middle of computational domain

The available experimental data obtained by Lacroix (1993) is chosen to validate the reliability of the numerical results. In Lacroix's experiment, PCM is n-Octadecane and HTF is water. The inner tube is plain and it is made of copper while the shell is made of plexiglass. Fig. 3 shows the comparison of the numerical and experimental results of temperature time trace at location  $T_1$  ( $z = 0.51$  m,  $r = 0.0099$  m) and  $T_2$  ( $z = 0.51$  m,  $r = 0.0089$  m) when the inlet temperature of HTF are 305.7 K and 310.7 K, respectively. As shown in Fig. 3, the maximum relative error between the numerical and experimental results is 0.52% at  $\tau = 5.5$  s. The results indicate that the numerical results agreed very well with those obtained experimentally by Lacroix.

### 4. RESULTS AND DISCUSSIONS

The thermal behavior and heat transfer characteristics of the corrugated tube phase change thermal energy storage unit during the charging and discharging processes are investigated in the following sections. For all the cases, the parameters used in this section are:  $q_m = 0.0315$  kg/s,  $r_i = 6.35$  mm,  $\delta = 1.55$  mm and  $L = 400$  mm. The dimensions of the inner tubes are selected to maintain the amount of the PCM constant for all the cases. The diameters of outer tubes increase with the increasing surface area of inner corrugated tubes for all the cases with respect to the case of plain tube.

#### 4.1 Comparison of plain and corrugated tube

Fig. 4 shows the contours of temperature during charging process in the corrugated tube-and-shell storage unit. The corrugated tube has a wavelength of  $h_{wave} = 3$ mm, a wave amplitude of  $w_{wave} = 16$ mm and outer cylindrical diameter  $r_o = 13.87$ mm. The initial temperature of

PCM and inlet temperature of HTF are set to 282.7 K and 310.7 K, respectively. The solid PCM around the HTF tube absorbs

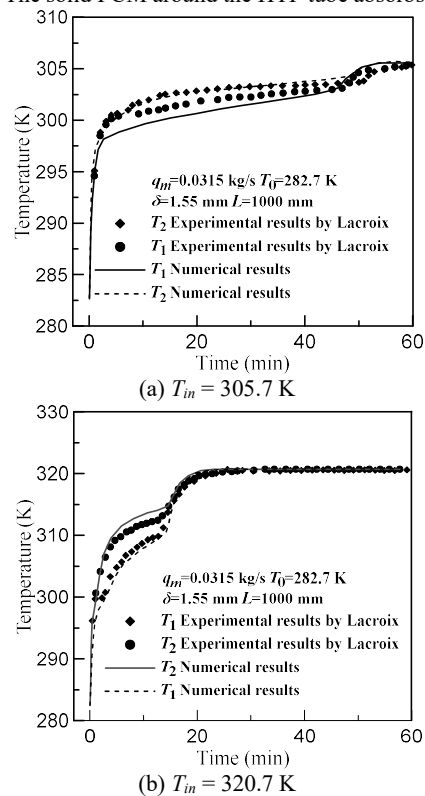


**Fig. 3** Comparisons of numerical and experimental results of temperature time trace at different locations for (a)  $T_{in} = 305.7$  K (b)  $T_{in} = 320.7$  K.

thermal energy from the hot HTF via the tube surface and starts melting when the temperature reaches the melting point. The isotherm varies along the corrugated tube wall at early stage and the temperature gradient is large nearby the HTF tube. At  $\tau = 10$  min, the value of average temperature is 302.9 K and the corresponding liquid fraction of PCM is 0.74. The value of PCM average temperature increases with time gradually and its value can rise up to 306.6 K at  $\tau = 20$  min. The PCM melt completely and the temperature of PCM at every point is approximate to the temperature of HTF after 30 minutes. Fig. 5 shows the contours of PCM temperature during discharging process in the corrugated tube-and-shell storage unit. The temperature field varies obviously due to the larger temperature difference of PCM and HTF. The corresponding temperature gradient is quite large nearby the tube wall. The direction of heat flux in discharging process is opposite to the direction of heat flux in charging process. The heat can be transferred from phase change material to heat transfer fluid. The charging time is longer than the discharging time. This is due to the charging process, initially the PCM is solid. Heat from the HTF is transferred to the PCM, then the solid of PCM becomes liquid. With the increase of time, the heat of HTF will be transferred to the solid of PCM through the liquid of PCM and the thermal resistance becomes larger. In the discharge process, initially the PCM is liquid. Heat from the PCM is transferred to the HTF and the liquid of PCM near the tube wall first becomes a solid. After that, the heat from PCM will be transferred to HTF through the PCM of solid with less thermal resistance.

Time signal of temperature at different locations ( $T_3$  (12.9 mm, 100 mm),  $T_4$  (12.9 mm, 692 mm),  $T_5$  (12.9 mm, 700 mm),  $T_6$  (10.9 mm, 700 mm)) for charging and discharging process are shown in Fig. 6 (a) and (b), respectively. In charging process, the values of temperature at four different locations vary dramatically up to the melting temperature at the beginning because of dominated action of thermal conduction. Then the change of temperature becomes slower due to the sensible heat

transfer in this period time of melting. Finally, the curve of temperature versus time became a straight line and the heat transfer in thermal energy storage unit arrived at steady-state. Although the distances of  $T_3$  and  $T_4$  from HTF inlet are different, the temperature curves at  $T_3$  and  $T_4$  with the same radial positions are almost the same. This is because that the change of HTF temperature is not obvious from inlet to outlet of tube. The difference of  $T_5$  and  $T_6$  is very obvious due to their different distance from HTF tube. The rates of the temperature increase for  $T_6$  nearby the HTF tube wall is higher than  $T_5$ . Similar conclusions can be obtained for the discharging process.

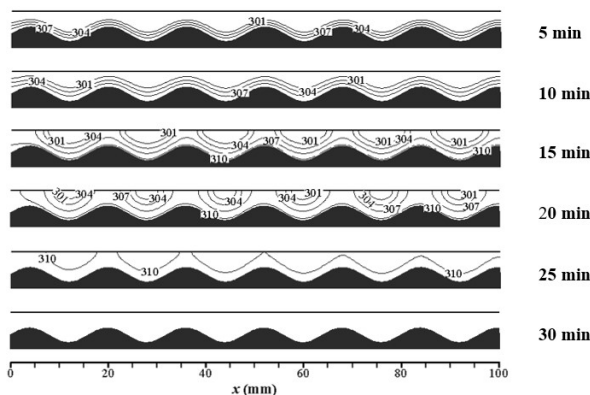


Fig. 4 PCM temperature fields with time during the charging process

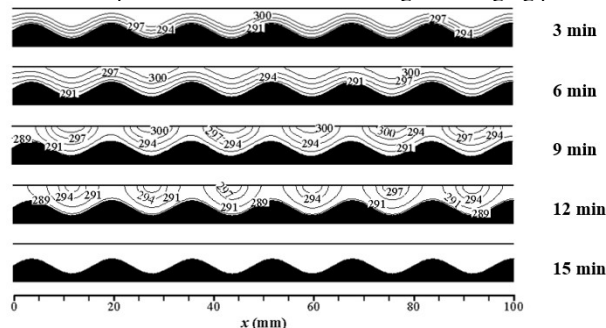


Fig. 5 PCM temperature fields with time during the discharging process.

Fig. 7 illustrates the evolution of heat transfer rates through the inside tube wall corrugated tube and plain tube while the inlet temperature is maintained at 310.7 K. It is found that the total discharging process costs shorter time than that of the corresponding charging process. In charging process, the heat of HTF will be transferred to the solid of PCM through the liquid of PCM. This will result in a reduced heat flux from the HTF to the solid of PCM due to the liquid of PCM has small thermal conductivity. In discharging process, the heat of PCM will be transferred to the HTF through the solid of PCM and the more heat of PCM will be transferred to the HTF through the solid of PCM. During charging process, heat transfer rates increase sharply and then decrease gradually after reaching a maximum value, as shown in Fig. 7(a). For the corrugated tube, the maximal value of heat transfer rate is about 1199 W but for plain tube, the maximal value of heat transfer rate is about 955 W. The time cost of heat transfer rate reaches nearly to zero can be reduced by 21.74% for the case of corrugated tube when it is compared with the case of plain tube. Correspondingly, the direction of heat transfer alters and the absolute value of heat transfer rate can arrive at the maximum value of 1185 W at the beginning and then gradually decrease after several minutes. The time cost of discharging process for the case of corrugated tube is reduced by 17.9% for the case of plain tube. Therefore, the heat transfer efficiency can be improved by the corrugated tube obviously for both the charging and discharging processes.

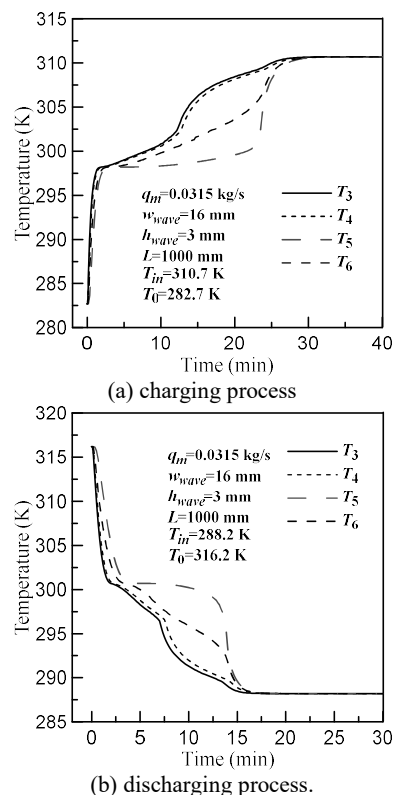


Fig. 6 Time signal of temperature at different locations ( $T_3$ (12.9mm, 100mm),  $T_4$  (12.9mm, 692mm),  $T_5$ (12.9mm, 700mm),  $T_6$  (10.9mm, 700mm)) for (a) charging process (b) discharging process.

#### 4.2 Effect of HTF inlet temperature and mass flow rate

The effect of mass flow rate on the heat transfer of PCM is studied for the geometric parameters of  $h_{wave} = 3\text{ mm}$  and  $w_{wave} = 16\text{ mm}$ . The values of initial temperature of PCM for charging and discharging processes are equal to 282.7 K and 316.2 K, respectively. Table 3 shows the charging and discharging time of PCM for different mass flow rates. When the mass flow rate increase from 0.00315kg/s to 0.0315 kg/s, the charging and discharging times reduce 17.12 min and 22.31 min, respectively. The charging and discharging time can be shorten, obviously. When the mass flow rate increase from 0.0315 kg/s to 0.315 kg/s, the charging and discharging times reduce 1.6 min and 0.8 min, respectively. However, it can also be seen from the table with the increase of mass flow rate from 0.315kg/s to 3.15 kg/s, the charging and discharging time can not be shorten obviously. It means the heat transfer rate is not improved significantly by increasing the flow rate because that the thermal resistance mainly exists in the PCM domain for the case of  $q_m > 3.15\text{ kg/s}$ . It can be deduced that the increase in mass flow rates to very high values does not necessarily lead to significant reduction in charging or discharging time.

The charging and discharging time of PCM under various HTF inlet temperatures are shown in Fig. 8. The mass flow rate is fixed on 0.0315 kg/s. When the temperature differences of HTF inlet and melting temperature is equal to 5 K, the charging time of charging process is 35.8 min, whereas at the higher temperature differences of 25 K, it only needs to take 9.5 min for the charging process. The charging time is reduced by 73.5% as the temperature differences increases from 5 K to 25 K. The corresponding discharging time can be reduced by 69.8% in the same range of temperature difference. Fig. 8 (b) shows the effects of the temperature differences on the discharging time. With temperature differences increase from 5 K to 25 K, the discharging time reduces from 21.5 min to 6.5 min, which reduces about 69.8%. The

results indicated that the heat transfer rate increases with the increasing temperature difference, the charging or discharging time can be shorted by increasing the HTF inlet temperature and initial PCM temperature.

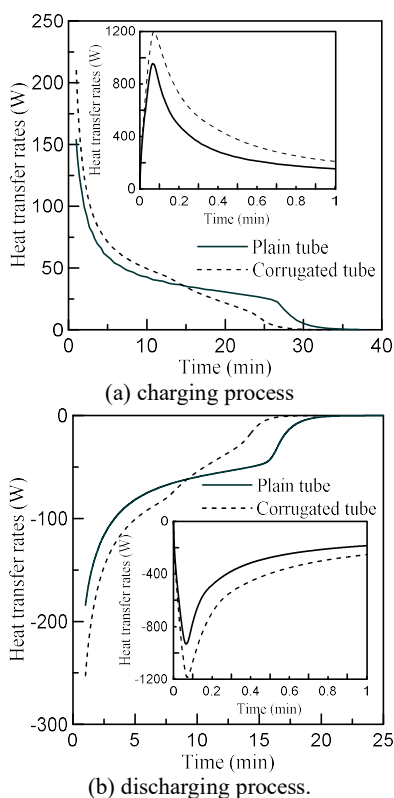


**Fig. 7** Time signal of heat transfer rate for charging and discharging process (a) charging process (b) discharging process

**Table 3** Comparison of charging and discharging time for different mass flow rate

	0.00315kg/s	0.0315kg/s	0.315kg/s	3.15kg/s
Charging time	37.53 min	23.1min	21.5min	21.3min
Discharging time	31.2min	12.5min	11.7min	11.5min

### 4.3 Effect of wavelength

The effects of the wavelengths on the heat transfer characteristics in thermal energy storage unit with corrugated tube are studied in this section. Fig. 9 shows the time signal of liquid fraction in charging and discharging processes for different wavelengths. The liquid fraction varies quite obvious at the early stage of charging process for all the values of wavelengths which is considered in this study. The change of liquid fraction becomes smaller with time gradually. When the liquid fraction is greater than 0.9 in charging process or less than 0.1 in discharging process, the charging or discharging rate is very slow. Figure 10 shows the charging and discharging time for different wavelengths. As is shown in this figure, the charging and discharging time become longer with the increasing wavelength due to the decrease in heat transfer surface. The heat transfer rate decreases in the range of 4mm to 16 mm obviously while the change of heat transfer rate become smaller for the case of  $w_{wave} > 32$  mm. The results indicate that the heat transfer rate can be improved by decreasing the wavelength because of the increasing heat transfer surface on the side of PCM domain.

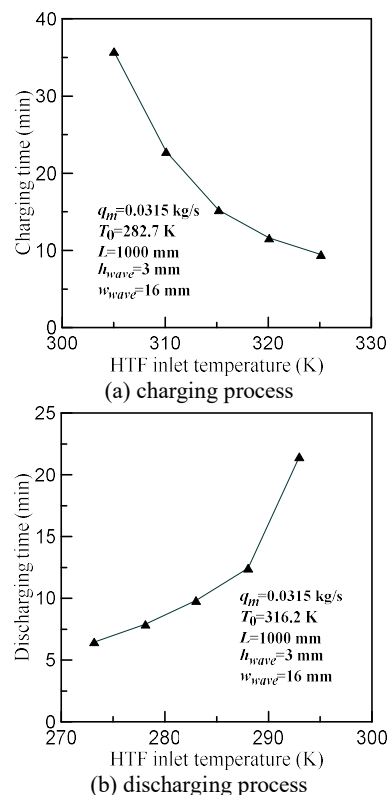


**Fig. 8** Comparison of charging and discharging time for different HTF inlet temperatures (a) charging process (b) discharging process

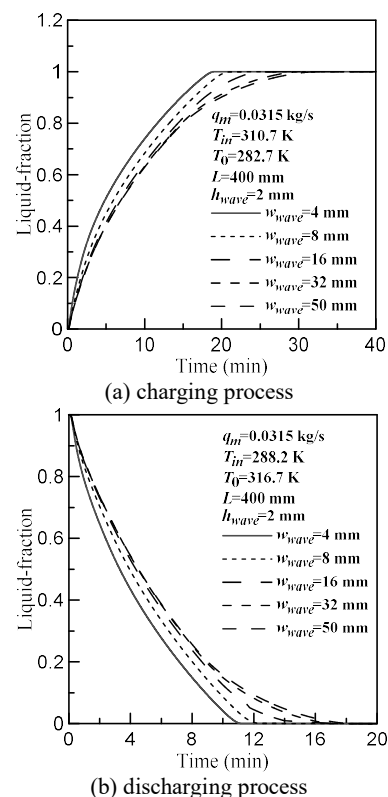


**Fig. 9** Time signal of liquid fraction for different wavelength for (a) charging process (b) discharging process

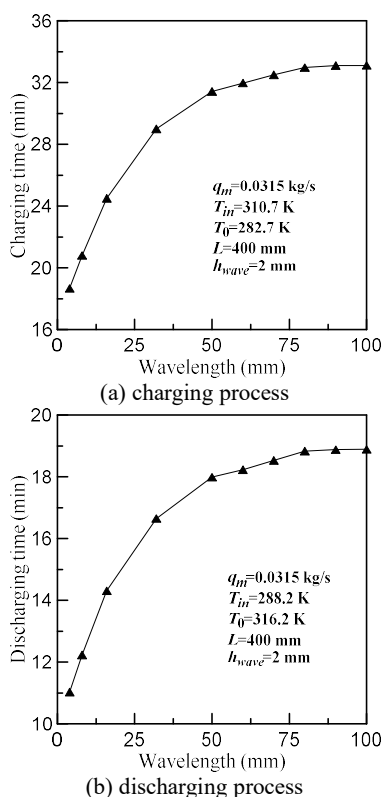


**Fig. 10** Charging and discharging time for different wavelengths (a) charging process (b) discharging process

#### 4.4 Effect of wave amplitude

In this section, the geometrical sizes which are chosen for these corrugated tubes are  $w_{wave} = 8$  mm,  $d_i = 12.7$  mm,  $\delta = 1.55$  mm and  $L = 400$  mm. Thermal energy storage unit with different wave amplitudes is studied in this section. The liquid fraction evolution for the charging and discharging processes under various wave amplitudes is shown in Fig. 11. The effect of wave amplitude on charging and discharging time of PCM is shown in Fig 12. It is observed that as the wave amplitude increases, the charging and discharging time is decreased. When the wave amplitude is equal to 2 mm, the charging time of charging process is 20.8 min, whereas at the higher wave amplitude of 6 mm, it only needs to take 12.2 min for the charging process. The charging time is reduced by 41.3% as the wave amplitude increases from 2 mm to 6 mm. Fig. 12 (b) shows the effects of the wave amplitude on the discharging time. When the values of wave amplitude increase from 2 mm to 6 mm, the discharging time reduces from 12.2 min to 7.5 min, which reduces about 38.5%. This is due to an increase of heat transfer rate caused by the increasing heat transfer surface of PCM and HTF tube.

#### 5. CONCLUSIONS

The charging and discharging processes of PCM in shell-and-tube storage unit were investigated simulated numerically. The PCM liquid fraction, heat transfer rate and temperature fields were studied with different HTF inlet temperatures, mass flow rate, wavelength and wave amplitudes. The conclusions can be obtained as follows.

The study showed that the corrugated wall can increase the surface of heat transfer, the melting rate of PCM in phase change thermal energy storage unit with corrugated is obviously higher than that in the unit with plain tube. Both charging and discharging time can be shorten for the phase change thermal storage unit with corrugated wall. The heat transfer rate increase with the increasing mass flow rate.

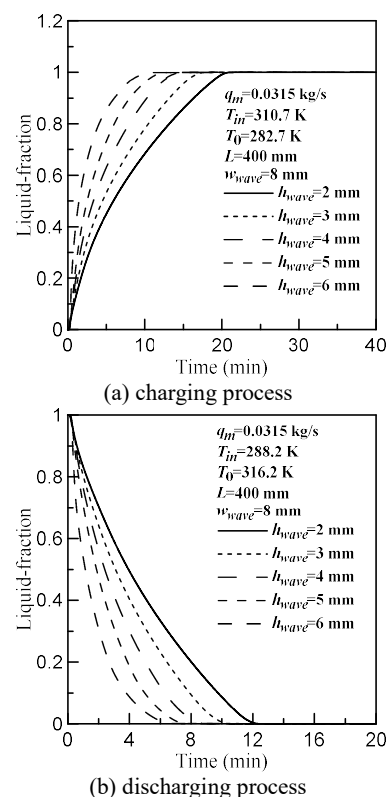


**Fig. 11** Time signal of liquid fraction with different wavelength for (a) charging process (b) discharging process

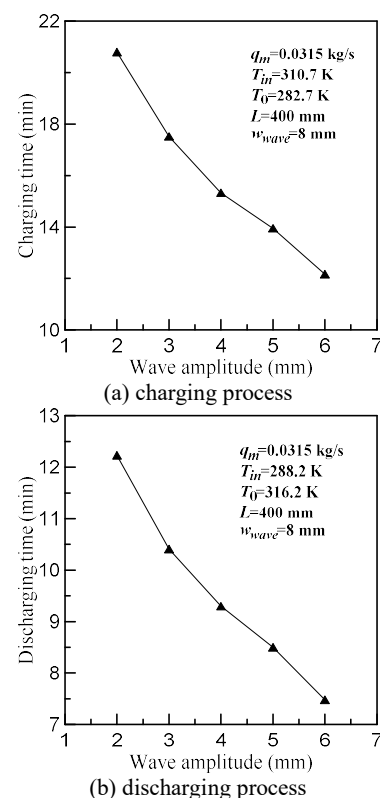


**Fig. 12** Charging and discharging time for different wave amplitudes (a) charging process (b) discharging process

However, when the mass flow rate of HTF is greater than 0.0315kg/s, the charge and discharge time can not be obviously shortened by increasing mass flow rate. The influences of wavelength and wave amplitude on the heat transfer of charging and discharging process need to be considered. The heat transfer rate increases with the decreasing wavelength and the increasing wave amplitude. Therefore, the efficiency of thermal energy storage can be enhanced by decreasing wavelength and inlet HTF temperature or increasing wave amplitude under the present parameters.

### ACKNOWLEDGEMENTS

The financial supports from the Chinese National Natural Science Foundation under Grants No.51866008 and Foundation of A Hundred Youth Talents Training Program of Lanzhou Jiaotong University are gratefully acknowledged.

### NOMENCLATURE

$A_{mush}$	mushy zone constant
$C$	constant in Eq. (5)
$C_p$	specific heat (J/kg·K)
$d_i$	inner diameter of the inner tube(mm)
$d_o$	outer diameter of the inner tube(mm)
$d_w$	diameter of the outer tube(mm)
$f$	the liquid phase number
$h_{wave}$	wave amplitude(mm)
$h$	enthalpy(J)
$H$	latent heat(J/kg)
$HTF$	heat conduction fluid
$k_e$	equivalence heat conduction coefficients(W/(m·K))
$k_{liq}$	liquid thermal conductivity(W/(m·K))
$k_p$	solid thermal conductivity(W/(m·K))
$L$	length of the thermal energy storage system(mm)
$n$	constant in Eq. (5)
$PCM$	phase change material
$q_m$	mass flow rate(kg/s)
$T_{in}$	HTF inlet temperatures(K)
$T_0$	PCM initial temperatures(K)
$w_{wave}$	wavelength(mm)
<b>Greek Symbols</b>	
$\rho$	density(kg/m <sup>3</sup> )
$\beta$	coefficient of thermal expansion(1/K)
$\delta$	thickness of corrugated tube(m)
$\mu_{pl}$	dynamic viscosity density(kg/(m·s))

### REFERENCES

Trp, A., 2005, "An experimental and numerical investigation of heat transfer during technical grade paraffin melting and solidification in a shell-and-tube latent thermal energy storage unit," *Solar Energy*, **79**(6), 648-660  
<https://doi.org/10.1016/j.solener.2005.03.006>

Trp, A., Lenic, K., and Frankovic, B., 2006, "Analysis of the influence of operating conditions and geometric parameters on heat transfer in water-paraffin shell-and-tube latent thermal energy storage unit," *Applied Thermal Engineering*, **26**(16), 1830-1839.  
<https://doi.org/10.1016/j.applthermaleng.2006.02.004>

Shukla, A., Buddhi, D., and Sawhney, R.L., 2009, "Solar water heaters with phase change material thermal energy storage medium: a review," *Renewable and Sustainable Energy Reviews*, **13**(8), 2119-2125.  
<https://doi.org/10.1016/j.rser.2009.01.024>

Amirante, R., Cassone, E., Distaso, E., and Tamburrano, P., 2017, "Overview on recent developments in energy storage: Mechanical,

electrochemical and hydrogen technologies," *Energy Convers Management*, **132**, 372-387.  
<https://doi.org/10.1016/j.enconman.2016.11.046>

Al-Obaidi, A.R., 2019, "Investigation of fluid field analysis, characteristics of pressure drop and improvement of heat transfer in three-dimensional circular corrugated pipes," *Journal of Energy Storage*, **26**, 101012.  
<https://doi.org/10.1016/j.est.2019.101012>

Ding, Z., Qi, C., Luo, T., Wang, Y., Tu, J., and Wang, C., 2022, "Numerical simulation of nanofluids forced convection in a corrugated double-pipe heat exchanger," *The Canadian Journal of Chemical Engineering*, **100**(8), 1554-1964.  
<https://doi.org/10.1002/cjce.24267>

Agyenim, F., Eames, P., and Smyth, M., 2009, "Heat transfer enhancement in medium temperature thermal energy storage system using a multitube heat transfer array," *Renewable Energy*, **35**(1), 198-207.  
<https://doi.org/10.1016/j.renene.2009.03.010>

Liang, H., Niu, J., and Gan, Y., 2020, "Performance optimization for shell-and-tube PCM thermal energy storage," *Journal of Energy Storage*, **30**, 101421.  
<https://doi.org/10.1016/j.est.2020.101421>

Wang, J., Ma, H., Zhu, Q., Dong, Y., and Yue, K., 2016, "Numerical and experimental investigation of pulsating heat pipes with corrugated configuration," *Applied Thermal Engineering*, **102**, 158-166.  
<https://doi.org/10.1016/j.applthermaleng.2016.03.163>

Ismail, K., Alves, C., and Modesto, M.S., 2001, "Numerical and experimental study on the solidification of PCM around a vertical axially finned isothermal cylinder," *Applied Thermal Engineering*, **21**(1), 53-77.  
[https://doi.org/10.1016/S1359-4311\(00\)00002-8](https://doi.org/10.1016/S1359-4311(00)00002-8)

Lacroix, M., 1993, "Numerical simulation of a shell-and-tube latent heat thermal energy storage unit," *Solar Energy*, **50**(4), 357-367.  
[https://doi.org/10.1016/0038-092X\(93\)90029-N](https://doi.org/10.1016/0038-092X(93)90029-N)

Mahkamov, K.K., 2006, "Solar energy storage using phase change materials," *Renewable and Sustainable Energy Reviews*, **11**(9), 1913-1965.  
<https://doi.org/10.1016/j.rser.2006.05.005>

Ming, F., and Chen, G., 2006, "Effects of different multiple PCMs on the performance of a latent thermal energy storage system," *Applied Thermal Engineering*, **27**(5), 994-1000.  
<https://doi.org/10.1016/j.applthermaleng.2006.08.001>

Hosseini, M.J., Ranjbar, A.A., Sedighi, K., and Rahimi, M., 2012, "A combined experimental and computational study on the melting behavior of a medium temperature phase change storage material inside shell and tube heat exchanger," *International Communications in Heat and Mass Transfer*, **39**(9), 1416-1424.  
<https://doi.org/10.1016/j.icheatmasstransfer.2012.07.028>

El-Shaarawi, M.A.I., Said, S.A.M., and Siddiqui, M.U., 2012, "New simplified correlations for aqua-ammonia intermittent solar-powered absorption refrigeration systems," *International Journal of Air-Conditioning and Refrigeration*, **20**(2), 1250008.  
<https://doi.org/10.1142/S2010132512500083>

Rathod, M.K., and Banerjee, J., 2012, "Experimental Investigations on Latent Heat Storage Unit using Paraffin Wax as Phase Change Material," *Experimental Heat Transfer*, **27**(1), 40-55.  
<https://doi.org/10.1080/08916152.2012.719065>

Hosseini, M.J., Rahimi, M., and Bahrapoury, R., 2013, "Experimental and computational evolution of a shell and tube heat exchanger as a

PCM thermal storage system,” *International Communications in Heat and Mass Transfer*, **50**, 128-136.

<https://doi.org/10.1016/j.icheatmasstransfer.2013.11.008>

Hosseini, M.J., Ranjbar, A.A., Rahimi, M., and Bahrampoury, R., 2015, “Experimental and numerical evaluation of longitudinally finned latent heat thermal storage systems,” *Energy & Buildings*, **99**, 263-272.

<https://doi.org/10.1016/j.enbuild.2015.04.045>

Esapour, M., Hosseini, M.J., Ranjbar, A.A., and Bahrampoury, R., 2016, “Numerical study on geometrical specifications and operational parameters of multi-tube heat storage systems,” *Applied Thermal Engineering*, **109**, 351-363.

<https://doi.org/10.1016/j.applthermaleng.2016.08.083>

Maike, J., Stefan, H., Markus, B., Claudia, M., Michael, F., Bernd, H., Manfred, S., and Markus, E., 2018, “Assembly and attachment methods for extended aluminum fins onto steel tubes for high temperature latent heat storage units,” *Applied Thermal Engineering*, **144**, 96-105.

<https://doi.org/10.1016/j.applthermaleng.2018.08.035>

Kousha, N., Rahimi, M., Pakrouh, R., and Bahrampoury, R., 2019, “Experimental investigation of phase change in a multitube heat exchanger,” *Journal of Energy Storage*, **23**, 292-304.

<https://doi.org/10.1016/j.est.2019.03.024>

Qaiser, R., Khan, M.M., Lehar, A., Khan, and Irfan, M., 2021, “Melting performance enhancement of PCM based thermal energy storage system using multiple tubes and modified shell designs,” *Journal of Energy Storage*, **33**, 102161.

<https://doi.org/10.1016/j.est.2020.102161>

Qi, C., Luo, T., Liu, M., Fan, F., and Yan Y., 2019, “Experimental study on the flow and heat transfer characteristics of nanofluids in double-tube heat exchangers based on thermal efficiency assessment,” *Energy Conversion and Management*, **197**, 111877.

<https://doi.org/10.1016/j.enconman.2019.111877>

Kumar, R., and Verma, P., 2020, “An experimental and numerical study on effect of longitudinal finned tube eccentric configuration on melting behaviour of lauric acid in a horizontal tube-in-shell storage unit,” *Journal of Energy Storage*, **30**, 101396.

<https://doi.org/10.1016/j.est.2020.101396>

Ruihuan, G., Gabriele, H., Rafael, M., Moataz, M.A., and Adriano, S., 2020, “Additive manufacturing of a topology-optimised multi-tube energy storage device: Experimental tests and numerical analysis,” *Applied Thermal Engineering*, **180**, 115878.

<https://doi.org/10.1016/j.applthermaleng.2020.115878>

Mazhar, A.R., Liu, S., and Shukla, A., 2021, “Numerical investigation of the heat transfer enhancement using corrugated pipes in a PCM for grey water harnessing,” *Thermal Science and Engineering Progress*, **23**, 100909.

<https://doi.org/10.1016/j.tsep.2021.100909>

Yarmohammadi, S., and Farhadi, M., 2016, “Optimization of thermal and flow characteristics of R-404A vapor condensation inside corrugated tubes,” *Experimental Thermal and Fluid Science*, **79**, 1-12.

<https://doi.org/10.1016/j.exptthermfluidsci.2016.06.012>

Park, S.H., Yong, G.P., and Man, Y.H., 2020, “A numerical study on the effect of the number and arrangement of tubes on the melting performance of phase change material in a multi-tube latent thermal energy storage system,” *Journal of Energy Storage*, **32**, 101780.

<https://doi.org/10.1016/j.est.2020.101780>

Gang, S.A., Xw, A., Ac, A., Feng, C.B., and Xiang, Y.B., 2020, “Investigation on optimal shell-to-tube radius ratio of a vertical shell-and-tube latent heat energy storage system,” *Solar Energy*, **211**, 732-743.

<https://doi.org/10.1016/j.solener.2020.10.003>

Yang, X., Wei, P., Cui, X., Jin, L., and He, Y.L., 2019, “Thermal response of annuli filled with metal foam for thermal energy storage: An experimental study,” *Applied Energy*, **250**, 1457-1467.

<https://doi.org/10.1016/j.apenergy.2019.05.096>

Xu, Y., Zheng, Z.J., Chen, S., Cai, X., and Yang, C., 2021, “Parameter analysis and fast prediction of the optimum eccentricity for a latent heat thermal energy storage unit with phase change material enhanced by porous medium,” *Applied Thermal Engineering*, **186**, 116485.

<https://doi.org/10.1016/j.applthermaleng.2020.116485>

Tao, Y.B., He, Y.L., and Qu, Z.G., 2012, “Numerical study on performance of molten salt phase change thermal energy storage system with enhanced tubes,” *Solar Energy*, **86**(5), 1155-1163.

<https://doi.org/10.1016/j.solener.2012.01.004>

Tao, Y.B., Liu, Y.K., and He, Y.L., 2017, “Effects of PCM arrangement and natural convection on charging and discharging performance of shell-and-tube LHS unit,” *International Journal of Heat and Mass Transfer*, **115**, 99-107.

<https://doi.org/10.1016/j.ijheatmasstransfer.2017.07.098>

Li, Y.J., Wu, S.Q., and Jin, T., 2017, “Numerical study on the flow and heat transfer characteristics of slush nitrogen in a corrugated pipe,” *IOP Conference Series: Materials Science and Engineering*, **278**(1), 012131.

<https://doi.org/10.1088/1757-899X/278/1/012131>

Zhang, Y., Zhou, F., and Kang, J., 2020, “Flow and heat transfer in drag-reducing polymer solution flow through the corrugated tube and circular tube,” *Applied Thermal Engineering*, **174**, 115185.

<https://doi.org/10.1016/j.applthermaleng.2020.115185>

Gong, Z.X., and Mujumdar, A.S., 1996, “Cyclic heat transfer in a novel storage unit of multiple phase change materials,” *Applied Thermal Engineering*, **16**(10), 807-815.

[https://doi.org/10.1016/1359-4311\(95\)00088-](https://doi.org/10.1016/1359-4311(95)00088-)